

**Supporting Information**

**Highly active and stable Ni/ $\gamma$ -Al<sub>2</sub>O<sub>3</sub> catalysts selectively  
deposited with CeO<sub>2</sub> for CO methanation**

Qing Liu,<sup>a</sup> Jiajian Gao,<sup>a</sup> Meiju Zhang,<sup>a</sup> Huifang Li,<sup>a</sup> Fangna Gu,<sup>a,\*</sup>

Guangwen Xu,<sup>a</sup> Ziyi Zhong,<sup>b</sup> and Fabing Su<sup>a,\*</sup>

<sup>a</sup> *State Key Laboratory of Multiphase Complex Systems, Institute of Process Engineering, Chinese Academy of Sciences, Beijing, China 100190*

<sup>b</sup> *Institute of Chemical Engineering and Sciences, A\*star, 1 Pesek Road, Jurong Island, Singapore 627833*

\*Corresponding author. Tel.: +86 10 82544850; fax: +86 10 82544851. E-mail address:

fngu@ipe.ac.cn (F. Gu); fbsu@ipe.ac.cn (F. Su).

### S-1. Preparation of catalysts with 20 wt% NiO loading

20NiA was prepared by the wet impregnation method similar with the 40NiA. 3.89 g of  $\text{Ni}(\text{NO}_3)_2 \cdot 6\text{H}_2\text{O}$  was dissolved in 30 mL deionized water, then 4.00 g  $\gamma\text{-Al}_2\text{O}_3$  support (after the pretreatment at 400 °C, 2h) was added to form a slurry, and the rest procedures were the same with those of 40NiA. The procedures of 20NiAxC (x=1, 3 and 5), 20NiA3C-CI and 20NiA3C-SI which were prepared by deposition-precipitation (DP), co-impregnation (CI) and sequential impregnation (SI) methods respectively were also same with those of the 40 wt% NiO loading catalysts except the different  $\text{CeO}_2$  loading.

### S-2. Characterization data of catalysts with 20 wt% NiO loading

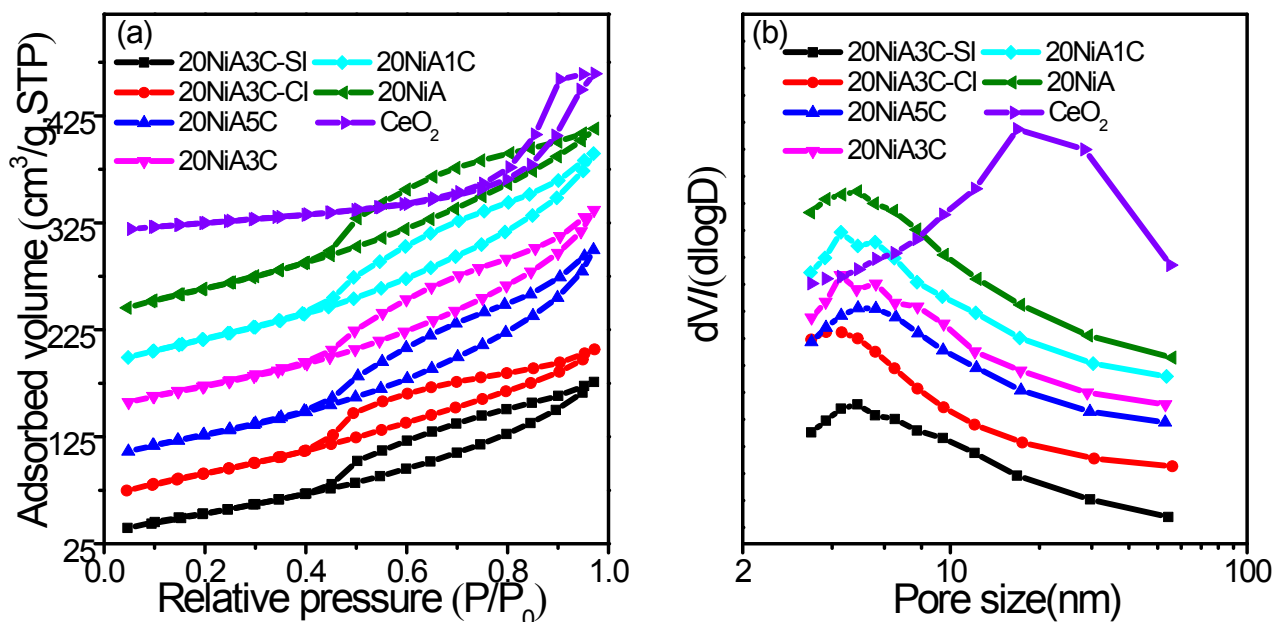


**Fig. S1** N<sub>2</sub> adsorption isotherms (a) and pore size distribution curves (b) of unreduced catalysts (For clarity, the isotherm of 20NiA3C-CI, 20NiA5C, 20NiA3C, 20NiA1C, 20NiA and CeO<sub>2</sub> was vertically shifted for 35, 70, 115, 155, 200 and 300 cm<sup>3</sup> g<sup>-1</sup>, respectively).

**Table S1** Physical property of the catalysts and CeO<sub>2</sub>.

Samples	$S_{\text{BET}}^a$ (m <sup>2</sup> g <sup>-1</sup> )	$V^b$ (cm <sup>3</sup> g <sup>-1</sup> )
CeO <sub>2</sub>	88	0.25
20NiA	229	0.33
20NiA1C	224	0.36
20NiA3C	245	0.34
20NiA5C	236	0.36
20NiA3C-CI	204	0.27
20NiA3C-SI	193	0.27

<sup>a</sup> Surface area of the unreduced catalysts, derived from BET equation.

<sup>b</sup> Pore volume of the unreduced catalysts, obtained from the volume of nitrogen adsorbed at the relative pressure of 0.97.

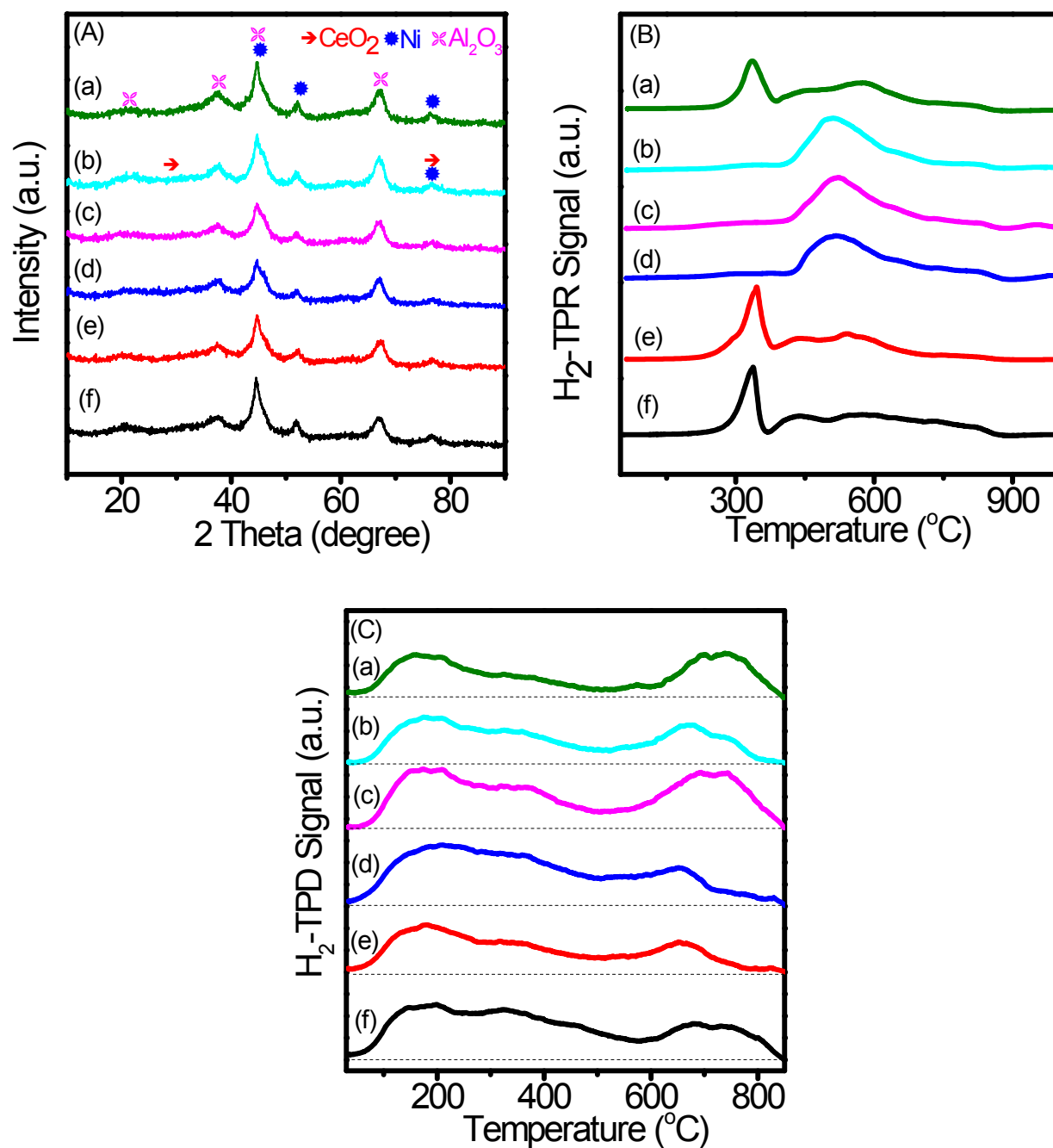


**Fig. S2** XRD patterns (A), H<sub>2</sub>-TPR profiles (B) and H<sub>2</sub>-TPD profiles (C): (a) 20NiA, (b) 20NiA1C, (c) 20NiA3C, (d) 20NiA5C, (e) 20NiA3C-CI, and (f) 20NiA3C-SI.

**Table S2** Chemical properties of the catalysts.

Samples	Ni Particle size (nm) <sup>a</sup>	H <sub>2</sub> uptake <sup>b</sup> (μmol·g <sup>-1</sup> )	D <sup>c</sup> (%)
---------	------------------------------------	--	--------------------

20NiA	5.4	127.8	9.55
20NiA1C	3.9	134.2	10.12
20NiA3C	3.8	190.9	14.70
20NiA5C	3.9	189.7	14.82
20NiA3C-CI	4.9	122.8	9.46
20NiA3C-SI	5.3	188.0	14.48

<sup>a</sup> Calculated by the XRD diffraction peak ( $2\theta=44.64^\circ$ ) using the Debye-Scherrer equation.

<sup>b</sup> Calculated based on the H<sub>2</sub>-TPR and H<sub>2</sub>-TPD results.

<sup>c</sup> Ni dispersion, calculated based on the H<sub>2</sub>-TPR and H<sub>2</sub>-TPD results.

### S-3. Catalytic measurement of catalysts with 20 wt% NiO loading

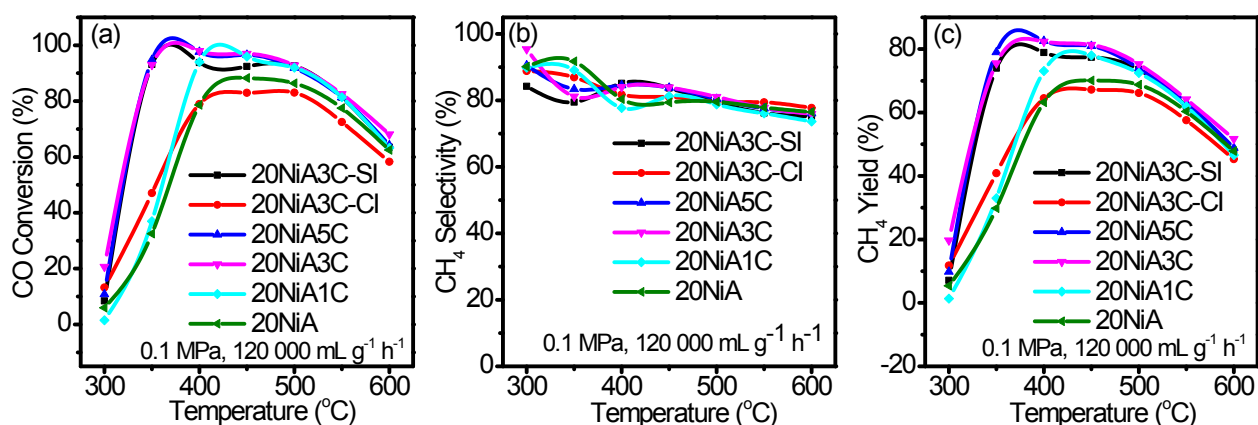


**Fig. S3** Catalytic properties of the different catalysts: (a) CO conversion, (b) CH<sub>4</sub> selectivity, and (c) CH<sub>4</sub> yield.

#### S-4. Life time test of 40NiA5C catalyst

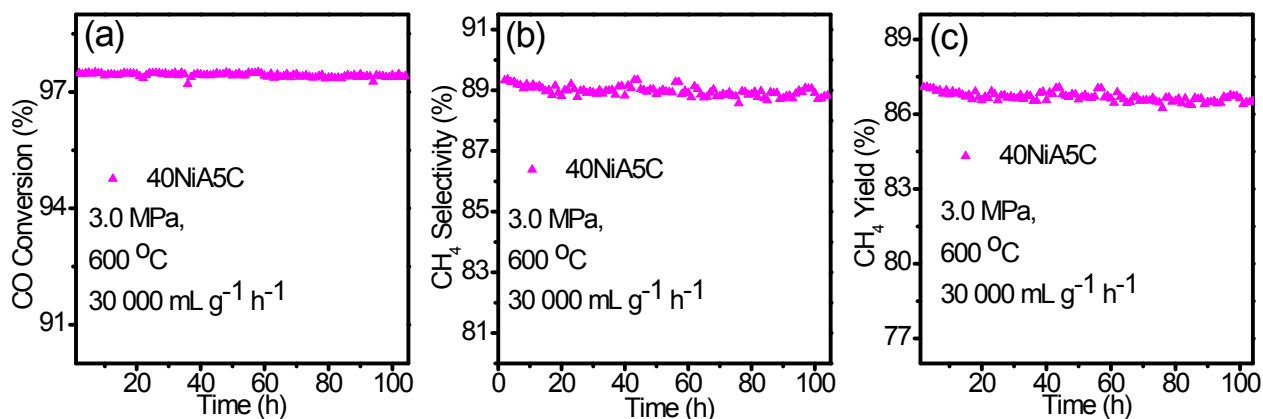


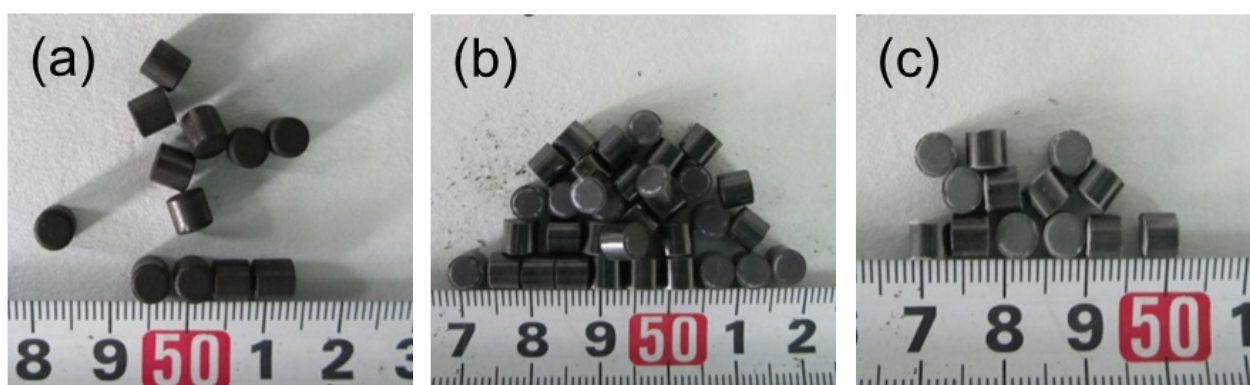
Fig. S4 Life time test of 40NiA5C: (a) CO conversion, (b) CH<sub>4</sub> selectivity, and (c) CH<sub>4</sub> yield.

#### S-5. Catalyst molding

In order to evaluate whether 40NiA5C can meet the requirement of industry, 40NiA5C and 40NiA are molded by a tablet press machine (Guangzhou Saihao Machinery Co., Ltd. China) with particle size of  $\Phi 5 \times 4$  mm. It should be pointed out that 3 wt% graphite (G)<sup>1</sup> (Qingdao Guyu Graphite Co., Ltd. China) is added as the lubricant and the catalysts molded are denoted 40NiA-G and 40NiA5C-G (Fig. S5). It can be seen the morphology of the three catalysts are very similar.

Crushing strength is an important parameter for the industry catalyst. Radial crushing strength and axial crushing strength are determined on a ZQJ-II Intelligent particle strength testing machine (Dalian Intelligent Testing Machine Factory, China), and the results are listed in Table S3. The radial crushing strength of 40NiA5C-G and 40NiA-G are a little higher than that of HT-1, and the axial crushing strength of the three catalysts are all over the range of testing machine.

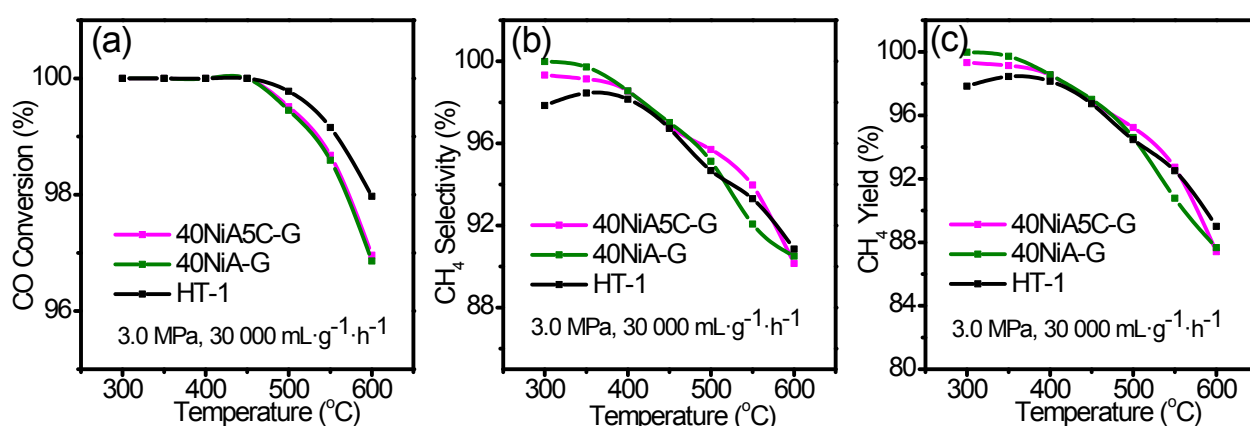
The molded catalysts are crushed and sieved into granules with a size of 20–40 meshes, and CO methanation over the crushed catalysts is carried out at 3.0 MPa and a WHSV of 30000 mL g<sup>-1</sup> h<sup>-1</sup>, the results are listed in Fig. S6. It can be seen that the activities of molded catalysts are close with those of HT-1, especially, the CH<sub>4</sub> yield of 40NiA5C-G can be higher than that of HT-1 in the temperature range of 300–550 °C, indicating the activity of 40NiA5C is still very high after molding.



**Fig. S5** Photos of the molded catalysts: (a) HT-1, (b) 40NiA-G, and (c) 40NiA5C-G.

**Table S3** Crushing strength of the molded catalysts.

Samples	Radial crushing strength (N cm <sup>-1</sup> )	Axial crushing strength (MPa)
HT-1	244	> 25.5
40NiA-G	252	> 25.5
40NiA5C-G	248	> 25.5

**Fig. S6** Catalytic properties of the different catalysts: (a) CO conversion, (b) CH<sub>4</sub> selectivity, and (c) CH<sub>4</sub> yield.

### S-6. Stability analysis of 40NiA catalyst

The photos of 40NiA catalyst bed before and after the life time test are shown in Fig. S7. In the life time test, 0.05 g 40NiA diluted with 2.5 g quartz sands is uploaded in quartz tube and then 0.5 g quartz sands are uploaded on the top of the catalyst bed as the air distributor (Fig. S7a). After the test, the wall of the tube above the catalyst bed is black for the carbon deposition (Fig. S7b). The coke on the wall is loose and can be wiped off by cotton easily (Fig. S7c), while the coke just no the

top of the catalyst bed in Fig. S7d is very hard and can only be wiped off by hard object. Therefore, the clog of the tube should occur on the top rather than the whole catalyst bed.

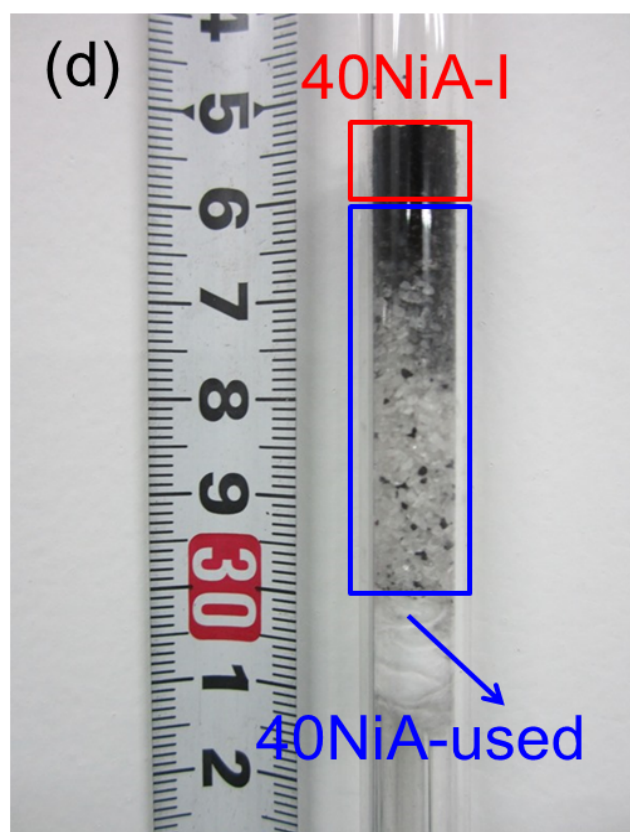
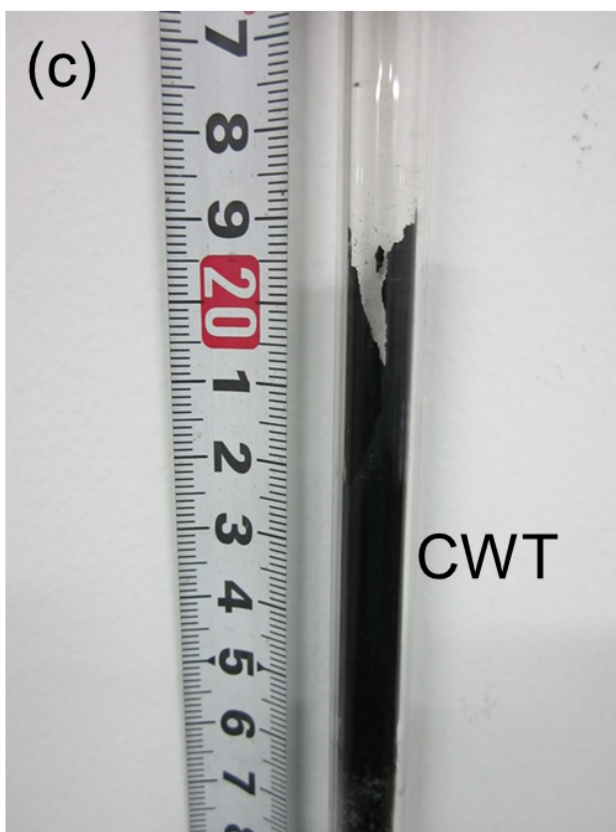
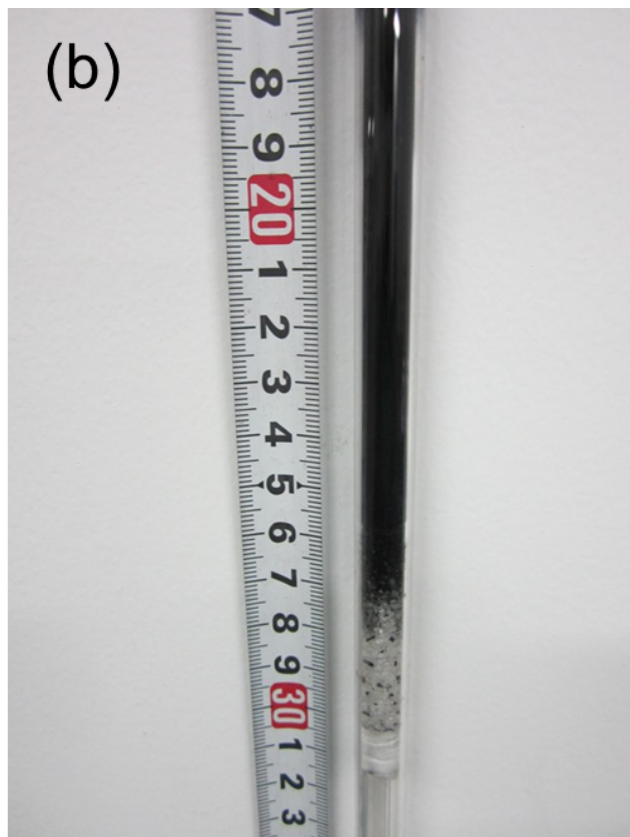
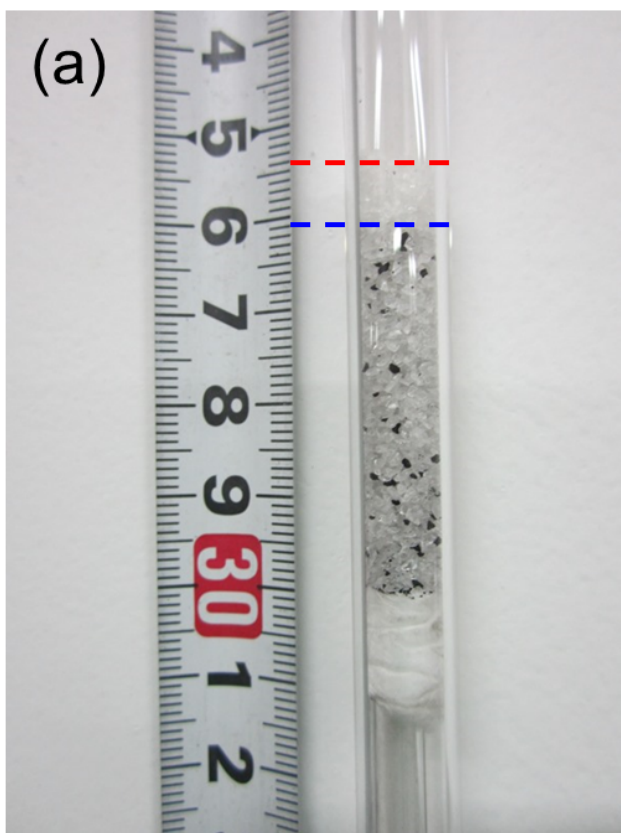


**Fig. S7** Photos of catalyst layer in the quartz tube: (a) before and (b) after the life time test, carbon deposition on the wall was erased partially (c) and totally (d) with the cotton.

The recycling 40NiA catalyst is also characterized by TEM and XRD. The recycled catalyst is divided to three sections, one is 40NiA-used which is recycled from the catalyst bed; the second is recycled from the interface of the catalyst bed which is denoted 40NiA-I; the third is the carbon on the wall of the tube which is denoted CWT. The TEM images of the recycling catalysts are shown in Fig. S8a–c. For 40NiA-used, few carbon filaments can be seen on the TEM image (Fig. S8a), and the carbon diffraction peak on the XRD pattern is very weak (Fig. S8d), which indicates that there is small amount of graphitic carbon on 40NiA-used. On the contrary, the 40NiA-I is almost totally composed by carbon filaments, only very few catalysts can be seen on its TEM image (Fig. S8b), indicating there is serious coke on the top (interface) of the catalyst bed. The Ni particle is observed to be encapsulated in the tip of filamentous carbon, whose structure is well consistent with the growth mechanism suggested by the literatures.<sup>2</sup> Additionally, the Ni particle size of 40NiA-I is 18.4 nm, a little bigger than that of 40NiA-used 17.9 nm, which also indicates that the temperature at the interface of the catalyst bed is higher. On the other hand, only carbon filaments can be seen in the TEM image of CWT (Fig. S8c), and there is no Ni diffraction peak in the XRD pattern of CWT, indicating that CWT is produced by CO Boudouard reaction without the catalysis of Ni particle. Therefore, the high temperature and the catalytic effect of Ni particle will aggravate the formation of deposited carbon on the top of the catalyst bed, which results in the clog of the quartz tube.

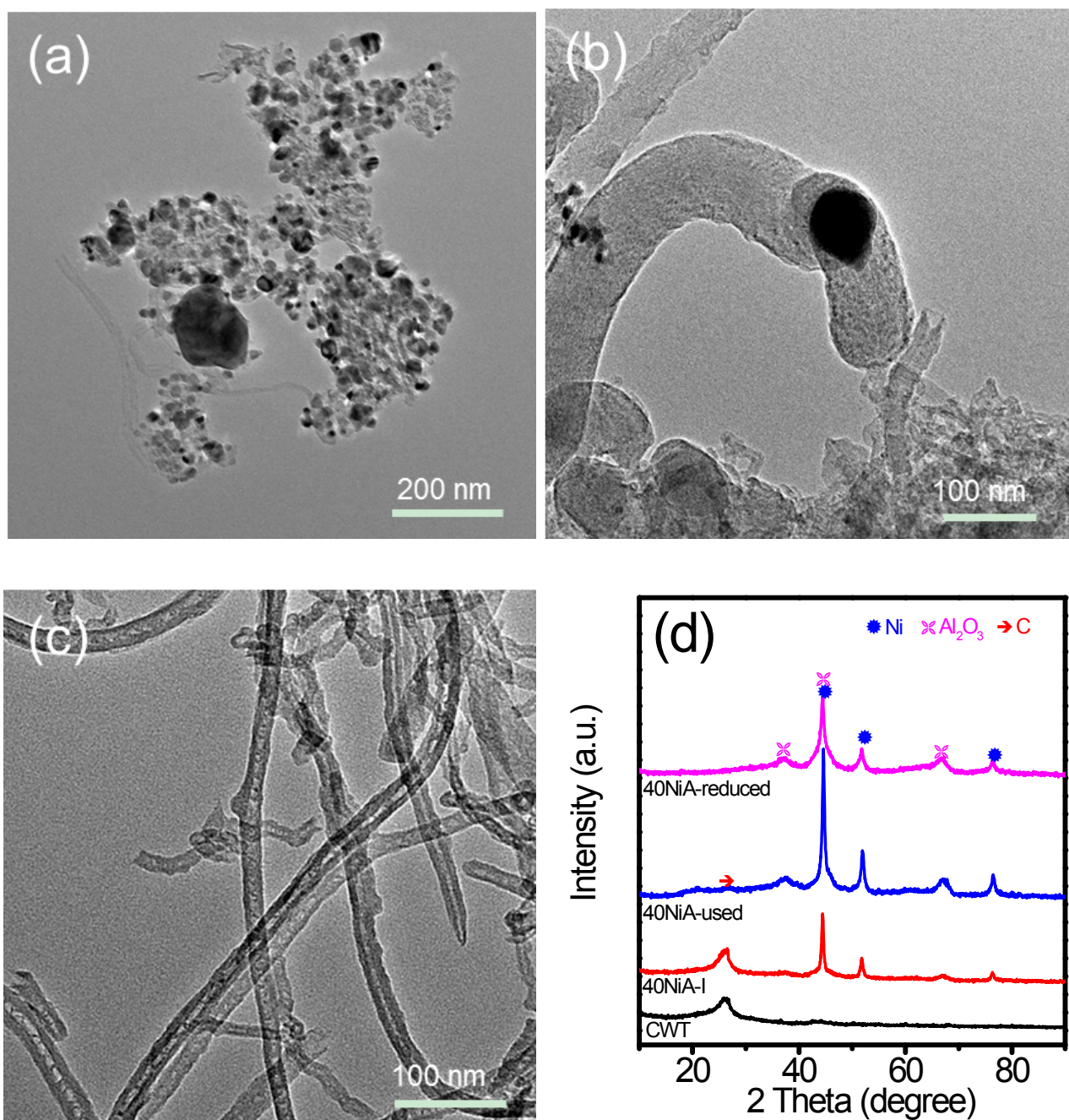


**Fig. S8** TEM images: (a) 40NiA-used, (b) 40NiA-I, (c) CWT, and XRD patterns of the 40NiA catalysts of reduced and recycled (a-c).

### S-7. Blank quartz tube test

It can be seen that the wall of the top of the catalyst bed is black, while that of the catalyst bed is still clear or semitransparent after the life time test (Fig. S7). In order to explain the above

experimental phenomena, two blank tube tests are conducted. Firstly, a blank tube test is carried out at 600 °C, atmospheric pressure for 8 h with the gas-flow rate of 200 mL min<sup>-1</sup> (dry mixed gas), and the quartz cotton is placed at the bottom of the flat-temperature zone of the furnace (Fig. S9a–b). After the test, the whole tube is covered by deposited carbon, but the color depth is different from the top to the bottom. The color of the tube just above the quartz cotton (the flat-temperature zone of the furnace) is light (Fig. S9b), which is because the Boudouard reaction is an exothermal reaction and the high temperature have adverse effects on this reaction. Steam is usually added to the methanation reactor to avoid carbon deposition in some CO methanation processes,<sup>3</sup> so another blank tube test is carried out with the same conditions as the former test, while 5 g quartz sands are added and the mixed gas is bubbled into water (the wet mixed gas) (Fig. S9c–d). After the test, the tube is exactly the same with the one before test without any deposited carbon (Fig. S9d), indicating the steam can eliminate carbon. Therefore, the clear tube around the catalyst bed after the life time test is the reason for the carbon elimination of the steam produced by CO methanation.

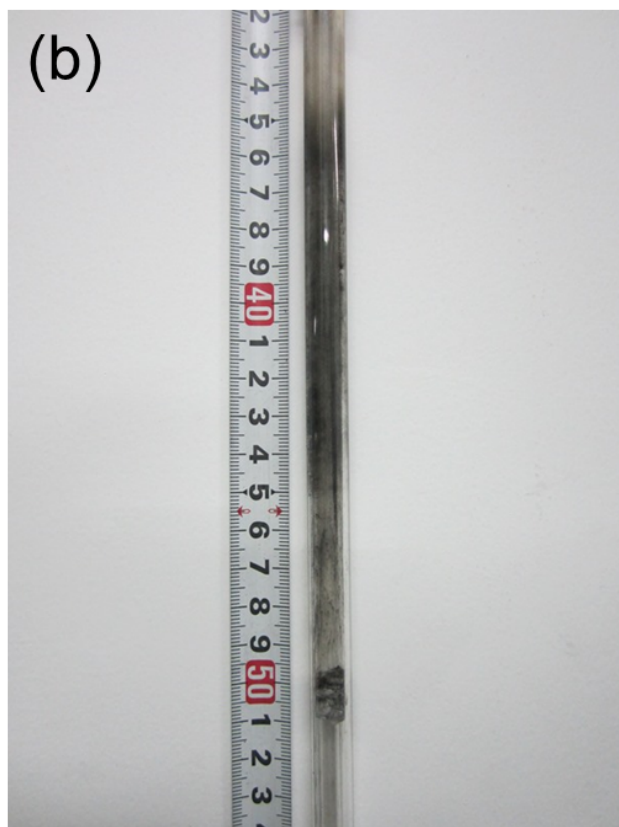
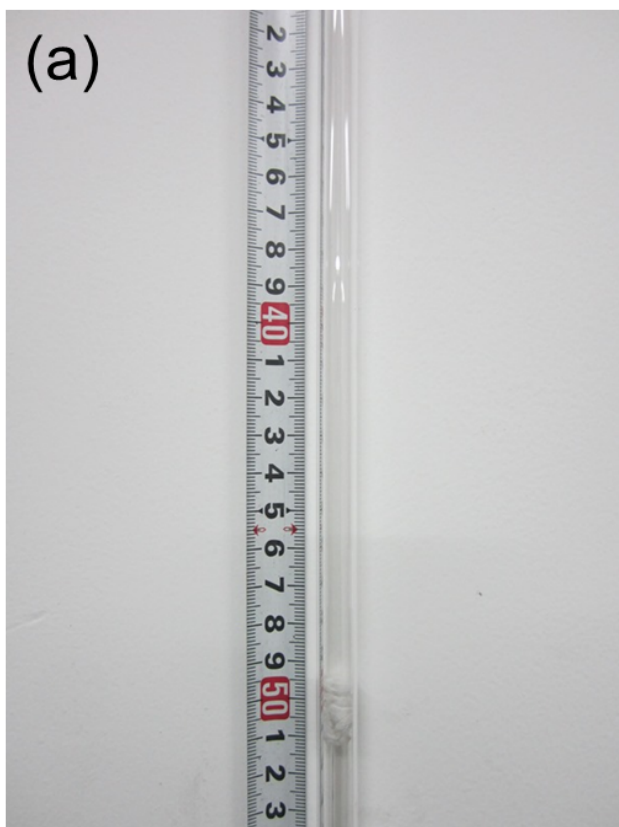


**Fig. S9** Photos of the quartz tube: (a) before and (b) after the blank tube test with dry mixed gas, and (c) before and (d) after the blank tube test with wet mixed gas.

## References

- 1 A. B. Stiles, Marcel Dekker New York, 1983, p. 58.
- 2 S. Helveg, C. Lopez-Cartes, J. Sehested, P. L. Hansen, B. S. Clausen, J. R. Rostrup-Nielsen, F. Abild-Pedersen and J. K. Norskov, *Nature*, 2004, **427**, 426-429.
- 3 J. Kopyscinski, T. J. Schildhauer and S. M. A. Biollaz, *Fuel*, 2010, **89**, 1763-1783.